(Received 18 November 2025, Accepted 4 January 2026, Scheduled 25 January 2026)

High-Efficiency Broadband GaN Power Amplifier with Algorithmic Gate-Bias Optimization

Ahmed Elrefaey[1], Fathi A. Faragb[2], Azhar A. Hamdi[2], and Amir Almslmany[1,*]

[1]*Department of Communications and Electronics Engineering, ADC, EMA, Cairo, Egypt*
[2]*Department of Electronics and Communications Engineering, Zagazig University, Zagazig, Egypt*

ABSTRACT: Achieving simultaneous wideband operation and high output power efficiency remains a major challenge in modern GaN HEMT power amplifier (PA) design, particularly for broadband communications and radar systems. This paper presents a systematic design methodology for a broadband PA that integrates radial-stub (RS)-based bias/matching networks with an algorithmic gate-bias (V_{GS}) optimization, alongside load-pull-derived device termination and compact layout. Starting with the Wolfspeed CMPA0530002S GaN HEMT, which features intrinsic broadband stability and an integrated input match, we replace conventional narrowband bias lines with a radial-stub network that ensures broadband bias isolation and low-loss matching. A thorough load-pull study identifies the optimum load impedance for concurrent maximization of power-added efficiency (PAE), gain, and output power. Subsequently, an automated V_{GS} sweep across the full 1.16–1.6 GHz band determines the optimal bias point for broadband and efficiency trade-off. The PA achieves a simulated result of output power of 34.28 dBm, flat gain of approximately 13.28 dB, and a peak PAE of 58.69% in a fractional bandwidth of 37% (1.16–1.6 GHz). A key novelty of this work lies in the proposed algorithmic V_{GS} sweep technique, which enables optimization of broadband efficiency throughout the entire 1.16–1.6 GHz operating band and can be easily extended to other frequency ranges. Unlike conventional bias optimization methods that are limited to a single frequency, the proposed algorithm systematically identifies the optimal gate bias across multiple frequencies to maintain high efficiency and consistent output power over a wide bandwidth. The simulated results confirm that this algorithmic bias optimization approach achieves superior broadband efficiency and stable output performance, providing a scalable and adaptable design methodology for next-generation wireless communication and electronic warfare systems.

1. INTRODUCTION

Nowadays, wireless communication systems are used in many different areas of life. They include 5G mobile networks, Wi-Fi 6/6E, satellite communications (especially in the L- and S-bands), military and civil radar systems (like L-band and S-band radars), GNSS (Global Navigation Satellite Systems) like GPS, and the Internet of Things and machine-to-machine (M2M) communication. Additionally, the signal bandwidth may be much larger, up to several hundred megahertz depending on the application [1–3]. One of the most critical components in radio frequency (RF) transmitter front-ends is power amplifier (PA), which largely determines the overall system performance in terms of bandwidth, output power, and efficiency. The proposed co-design method establishes a scalable and robust framework for next-generation high-efficiency broadband RF PA implementation [4, 5].

Thus, in order to satisfy the increasing demands of contemporary and upcoming wireless systems, the development of broadband PAs has become crucial. In response to the growing needs of contemporary wireless communication systems, a variety of design strategies have been studied recently to achieve wideband performance while retaining high efficiency and output power. Techniques such as continuous-mode operation (e.g., continuous Class-F [6], Quasi-Class-J [7], and continuous Class-J/F^{-1} [8]) have been frequently used to increase the bandwidth of intrinsic optimum impedances and reduce harmonic termination limitations.

Additionally, complex load modulation techniques, such as Doherty and outphasing architectures, have been carefully investigated and adjusted to improve broadband efficiency and performance over a large frequency range [9–11]. However, they frequently struggle to sustain appropriate load modulation over large bandwidths, exhibit higher complexity, and demonstrate reduced efficiency at power back-off. Furthermore, the literature has documented a number of filtering power amplifiers (FPAs) that seek to simultaneously combine high efficiency, wideband operation, and efficient out-of-band rejection [12].

To further enhance the bandwidth and efficiency of PAs, multi-section transmission-line transformers are commonly used to extend the matching bandwidth and improve impedance transformation [13]. However, their cascaded configuration often results in additional insertion loss, increased circuit size, and higher fabrication complexity, particularly at RF frequencies. To overcome these challenges, this work proposes a radial-stub (RS)-based matching network as an efficient alternative. By optimizing the stub geometry and simulated layout, the design achieves compact size, low loss, and ease of fabrication. The RS structure ensures smooth impedance transformation across a wide frequency range, providing

* Corresponding author: Amir Almslmany (dr.mslmany.7256.adc@alexu.edu.eg).

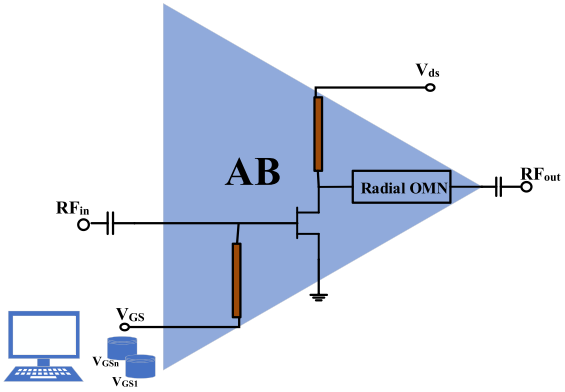

FIGURE 1. General block diagram of the proposed broadband power amplifier employing RS-based matching and gate-bias control.

stable performance, high efficiency, and strong tolerance to fabrication variations.

As shown in Figure 1, this paper presents an innovative methodology for designing a high-efficiency, wideband power amplifier (PA) utilizing a radial-stub (RS)-based matching network. Unlike the radial-stub implementations reported in [14, 15], which are primarily focused on monolithic microwave integrated circuit (MMIC)-based millimeter-wave applications or harmonic suppression purposes, the proposed work employs the radial-stub network as a fundamental wideband impedance-matching element for a high-power microstrip GaN PA. Moreover, a systematic and application-oriented simulation-based methodology is presented to ensure robust wideband performance and practical printed circuit board (PCB) realizability, rather than MMIC-specific or harmonic-tuning-oriented implementations. The RS topology provides wideband impedance matching while minimizing sensitivity to fabrication tolerances. Furthermore, to enhance the overall efficiency, an adaptive optimization algorithm is employed to determine the optimal gate bias voltage (V_{GS}). In this work, a novel algorithm is introduced to automatically identify the optimum V_{GS} across the entire broadband frequency range of 1.16–1.6 GHz. This approach enables consistent performance optimization over a wide bandwidth rather than at a single frequency, representing one of the key novelties of this study. The proposed bias optimization, while simple, provides a systematic and repeatable method for broadband PA design. The proposed algorithm achieves superior efficiency, making it highly applicable to next-generation broadband and high-efficiency RF PA designs.

The unique contributions of this work can be summarized as follows:

- The radial stub (RS) is employed as a broadband output matching and biasing element in a low-GHz high-power GaN power amplifier (PA) to achieve wideband impedance transformation and effective RF/DC isolation, rather than MMIC-based or filter-oriented applications as reported in [14–22].
- A frequency-averaged, algorithmic gate-bias optimization approach based on mean-value theory is utilized to identify a global optimum gate-source voltage (V_{GS}) across the entire operating bandwidth, instead of relying on single-frequency bias optimization.
- The main novelty of this work lies in the integrated use of RS-based broadband output matching with mean-theory-based broadband gate-bias optimization, enabling consistent and high-efficiency large-signal performance across the entire operating bandwidth.

The remainder of this paper is organized as follows. Section 1 presents the motivation, background, and related work on broadband GaN PA design. Section 2 discusses the theoretical basis and design methodology of the proposed RS based matching network combined with V_{GS} optimization for enhanced broadband efficiency. Section 3 describes the overall PA topology, including the integration of the optimized bias network and matching architecture. Section 4 reports the simulated performance, focusing on gain flatness, efficiency, and output power across the operating band. Section 5 provides a comparative assessment with recently reported state-of-the-art designs, highlighting the advantages of the proposed approach in terms of bandwidth and efficiency. Finally, Section 6 concludes the paper with a summary of the key findings and outlines future directions for experimental validation and implementation in high-efficiency broadband communication and electronic warfare systems.

2. RADIAL STUB NETWORKS WITH BIAS OPTIMIZATION FOR BROADBAND AND EFFICIENCY

The adoption of RS as matching elements in high PA design has proven to be a significant advancement over traditional rectangular stubs, particularly when broadband operation and high output power are required [16–18, 22]. Conventional stubs, while simple to implement, suffer from narrowband behavior and strong frequency sensitivity, which restrict their ability to provide stable impedance matching across wide operating ranges. In contrast, RS, with its sector-shaped geometry, inherently offers a lower characteristic impedance and a more forgiving frequency response, enabling more effective impedance transformation over multi-octave bandwidths. This property makes it especially suitable for broadband PAs, where consistent performance must be maintained across wide frequency spans [19, 21].

The radial stub (RS) used in the matching network can be analyzed as a series combination of an inductor and a capacitor. The input impedance Z_{in}, equivalent inductance L_r, and capacitance C_r can be approximately expressed as [23, 24]:

$$Z_{\mathrm{in}} \approx -j\,\frac{120\pi h\beta\theta_r}{\sqrt{\varepsilon_{eff}}}\left(\ln\frac{r_o}{r_i}+\frac{1}{2}+\frac{2}{\beta r_o^2}\right) \tag{1}$$

$$L_r = \frac{120\pi h}{\theta_r c}\left(\ln\frac{r_o}{r_i}-\frac{1}{2}\right) \tag{2}$$

$$C_r = \frac{\theta_r r_o^2 \varepsilon_{eff}}{240\pi h c} \tag{3}$$

where:

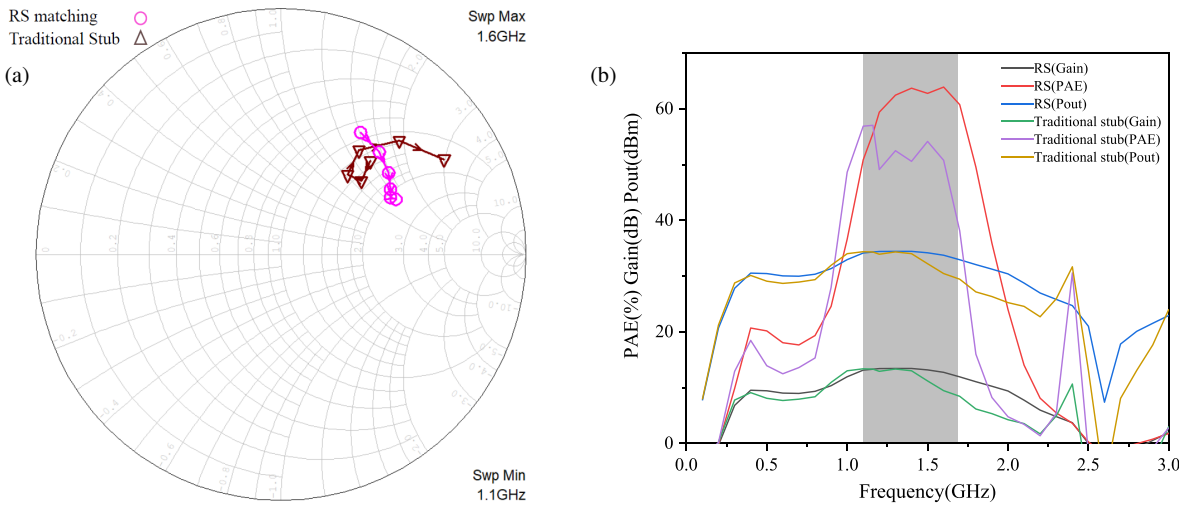

FIGURE 2. RS vs traditional stub. (a) Load impedance trajectory for RS and traditional stub. (b) O/P simulated result.

- h denotes the dielectric thickness;
- β represents the phase constant;
- θ_r is the spanning angle of the radial stub (in radians);
- c denotes the speed of light in free space;
- ε_{eff} represents the effective dielectric constant;
- r_i and r_o are the inner and outer radii of the radial stub, respectively.

From a practical standpoint, these characteristics allow RS to efficiently transform the inherent output impedance of a power transistor into the required load impedance. To support the impedance transformation claim, a Smith chart comparison between the proposed radial-stub (RS) matching network and a conventional open-stub network is presented over the 1.16–1.6 GHz band is presented, as shown in Figure 2(a). The impedance trajectories show that the RS network maintains impedance closer to the optimum load-pull solution, resulting in higher simulated PAE and improved large-signal performance, as shown in Figure 2(b). These observations are fully consistent with prior published work, such as [25], which demonstrates that radial stubs exhibit lower reactance variation than conventional stubs, leading to wider bandwidth and enhanced PA efficiency.

Recent innovations in RS design, such as sector-angle optimization and cascaded radial stubs, have been reported to improve impedance behavior, harmonic control, and overall PA efficiency [19, 20]. In the present work, these studies were analyzed and used as design guidance for the simulation-based RS output matching and biasing network, while the primary focus remains on exploiting the RS structure to enhance large-signal performance metrics (PAE, P_{out}, and P_{gain}) over the 1.16–1.6 GHz band. To further improve these performance metrics, algorithmic gate-bias optimization techniques are applied, allowing the nonlinear dependence of large-signal parameters on gate bias to be accurately captured and tuned. This method makes it possible to identify the optimum V_{GS} that maximizes efficiency, thereby ensuring that broadband amplifiers deliver superior gain, output power, and fidelity across wide frequency ranges [25].

The design and optimization of PAs demand a precise balance among key performance metrics such as broadband and efficiency to meet the stringent requirements of modern communication systems. Among the various design parameters, (V_{GS}) plays a decisive role in defining the transistor's operating characteristics and overall performance. By systematically sweeping V_{GS} and analyzing the corresponding efficiency datasets, designers can capture the nonlinear behavior of the device and identify the optimal bias point that maximizes PAE, P_{out}, and P_{gain} while ensuring stability [26, 27].

The visualized transistor behavior validates that the proposed design methodology — driven by precise tuning of V_{GS} — maximizes PAE at optimal P_{out} and P_{gain}. The transistor bias point is determined through the developed algorithm applied to the generated efficiency datasets. Specifically, the algorithm evaluates gate bias points within the Class-AB region, ranging from -1.65 V to -3.01 V in 0.01 V steps, corresponding to a total of 141 discrete V_{GS} values. The selected gate-source voltage sweep range from $V_{\text{GS}} = -1.65$ V to -3.01 V was chosen based on the transfer characteristics and biasing to ensure operation within the Class-AB region. Within this range, the transistor exhibits partial conduction over the RF cycle, providing an appropriate trade-off between linearity and efficiency.

Each of these 141 bias values represents the computed mean performance — averaged over the frequency range of 1.16 to 1.6 GHz.

As illustrated in Figure 3, Step A, three primary datasets are generated: the dataset of PAE $\{X\}$, the dataset of P_{out} $\{Y\}$, and the dataset of P_{gain} $\{Z\}$.

In Step B, the mean values of each dataset are computed based on the mean theory to establish representative performance levels for PAE, P_{out}, and P_{gain}. This step is a cornerstone of the proposed optimization algorithm, as it enables the evaluation of device performance across a broadband frequency range rather than at a single frequency point — constituting a primary novelty of this work. In this approach, frequency is defined as the independent variable on the x-axis, and each performance parameter, PAE(f), $P_{\text{gain}}(f)$, and $P_{\text{out}}(f)$, is modeled as a continuous function $F(x)$ over the frequency inter-

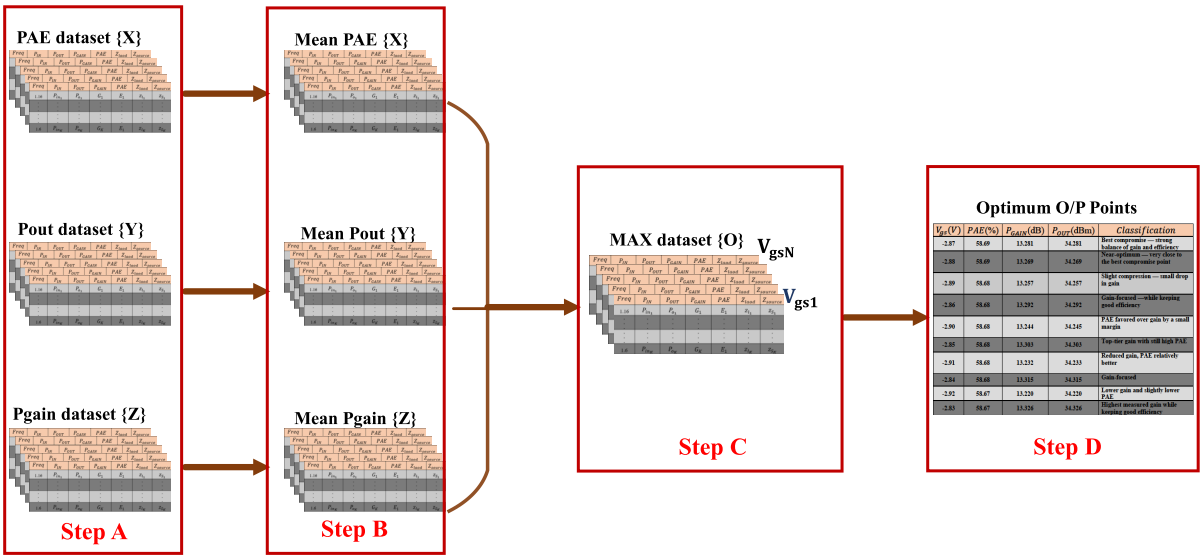

FIGURE 3. Proposed algorithm to determine the gate bias.

val [1.16, 1.6] GHz. The entire optimization process, including data fitting, integration, bias-voltage selection, and validation, is implemented through a dedicated Python-based algorithm that operates on frequency-dependent datasets extracted from Microwave Office environment (AWR) simulations, thus automating performance evaluation and confirming consistency between the analytical and simulated results.

According to mean theory, the representative mean value of each function within this interval is calculated using the fundamental relation [28]:

$$\bar{F} = \frac{1}{b-a}\int_a^b F(x)dx, \tag{4}$$

where a and b denote the lower and upper frequency limits, respectively. This operation provides a mathematically consistent way to extract the average broadband behavior of each dataset, ensuring that the optimization process reflects the global performance trend rather than localized variations. The resulting mean-based datasets are then constrained by the design criteria of $P_{\text{gain}} > 12\,\text{dB}$, PAE $> 55\%$, and $P_{\text{out}} > 34\,\text{dBm}$.

The intersection of these datasets, defined as $\{O\}$, represents the bias conditions that simultaneously satisfy all performance constraints across the broadband frequency range. This formulation establishes a systematic, frequency-averaged bias optimization method capable of identifying the most effective gate bias for achieving maximum PAE with respect to the optimum P_{out} and P_{gain} over a broadband range.

In Step C, the intersection dataset $\{O\}$ is further processed as a function of the gate bias voltage V_{GS} to identify the optimum bias condition that achieves the desired efficiency. For each discrete value of V_{GS}, the frequency-domain responses contained in $\{O\}$ are collected, and the frequency-averaged performance metrics are calculated according to the mean theory. The mean power-added efficiency (PAE), mean power gain (P_{gain}), and output power (P_{out}) are computed using the following mean-law relations:

$$\overline{\text{PAE}}(V_{\text{GS}}) = \frac{1}{b-a}\int_a^b \text{PAE}(f, V_{\text{GS}})df \tag{5}$$

$$\overline{P_{\text{gain}}}(V_{\text{GS}}) = \frac{1}{b-a}\int_a^b P_{\text{gain}}(f, V_{\text{GS}})df \tag{6}$$

$$\overline{P_{\text{out}}}(V_{\text{GS}}) = \frac{1}{b-a}\int_a^b P_{\text{out}}(f, V_{\text{GS}})df \tag{7}$$

where $[a, b] = [1.16, 1.6]$ GHz represents the operational frequency band. The optimization algorithm then forms a scalar objective function from these mean quantities, with whose help the optimal gate bias V_{GS}^* is determined.

Finally, in Step D, output points along with their performance parameters are derived from the algorithm and evaluated under the same design constraints, namely $P_{\text{gain},t} > 12\,\text{dB}$, $\text{PAE}_t > 55\%$, and $P_{\text{out},t} > 34\,\text{dBm}$. These points represent outcomes of the optimization process and are ranked according to their corresponding objective function values $S(V_{\text{GS}})$ to assess the robustness and consistency of the proposed mean-theory-based algorithm.

For the proposed broadband power amplifier design, the algorithm results show that the highest objective function value is achieved at $V_{\text{GS}} = -2.87\,\text{V}$, which provides maximum PAE with respect to the optimum P_{out} and P_{gain} over a broadband range. This procedure ensures that the selected bias point provides the best broadband efficiency while maintaining optimum P_{out} and P_{gain} over the frequency range of 1.16–1.6 GHz. This outcome verifies that the proposed algorithm can accurately detect the optimum bias point over a broadband frequency range rather than a single frequency, owing to its dependence on the mean value theory for frequency-domain averaging. Consequently, the optimum gate bias is not a localized value but a broadband-validated condition that ensures an enhanced maximum efficiency point. This demonstrates the reli-

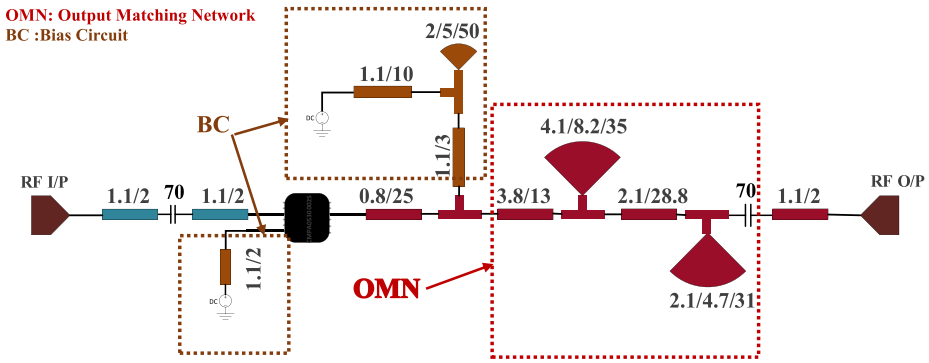

FIGURE 4. Proposed broadband PA, including RS-based output matching network and bias circuits.

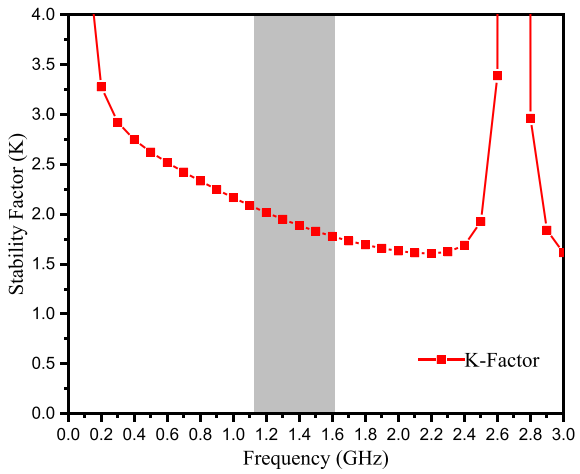

FIGURE 5. Stability curve.

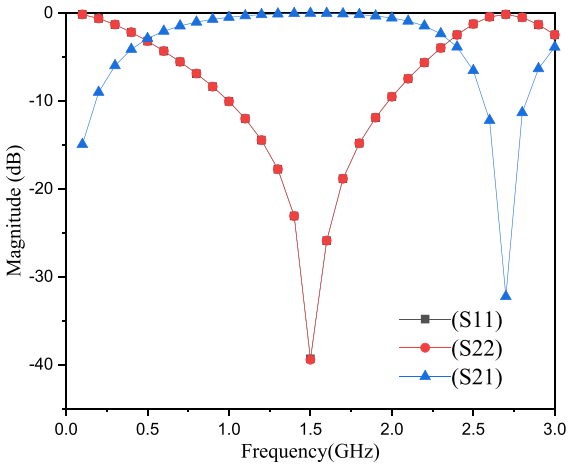

FIGURE 6. S parameter for RS bais tee.

ability and generality of the proposed broadband bias optimization methodology.

3. DESIGN METHODOLOGY AND SIMULATION OF THE PROPOSED PA

As shown in Figure 4, the proposed broadband PA employs the Wolfspeed CMPA0530002S Gallium Nitride (GaN) High Electron Mobility Transistor (HEMT) Monolithic Microwave Integrated Circuit (MMIC) as the active device. The device exhibits excellent thermal and electrical robustness, making it well-suited for high-power and wideband operation for its high efficiency and robustness in high-power applications. A notable feature of this device is its integrated input matching network, which reduces external circuit complexity, lowers input-stage insertion loss, and as shown in Figure 5, ensures stable performance across the target frequency band, eliminating the need for additional stabilization networks in most practical configurations that simplifies circuit integration. Proper biasing of the gate and drain terminals is essential for optimizing the efficiency of a PA.

To achieve stable biasing across a broad bandwidth, the design employs an RS-based bias tee. The RF-DC isolation provided by this radial-stub network has been quantitatively evaluated, as shown in the S-parameter plot included in Figure 6. Initial stub dimensions were determined using standard radial-stub theory as starting parameters and subsequently optimized numerically to achieve the desired broadband performance, ensuring both reproducibility and technical reliability. The gate-bias network, however, does not employ radial stubs because the selected MMIC GaN transistor inherently provides separate terminals for DC and RF at the gate — DC bias is applied to the dedicated DC path while the RF signal enters through the RF input terminal — ensuring good input matching and intrinsic stability across the operating band, which makes additional radial stubs unnecessary for the gate-bias network [29, 30].

To achieve optimum signal performance, a comprehensive load-pull simulation was conducted to evaluate the transistor's behavior across a wide impedance space. As shown in Figure 7, the frequency-dependent optimal load impedances over the 1.16–1.6 GHz band are clustered around $Z_{\text{opt}} = 154 + j10\,\Omega$, representing the best compromise among PAE, P_{out}, and P_{gain} across the operating band.

Following this, algorithmic sweep of V_{gs} was performed under Class-AB operation to examine the effect of bias variation on the device's nonlinear response and output capability. The Class-AB region was selected due to its inherent ability to maintain a favorable trade-off between efficiency and linearity, which is critical for broadband high-power applications. Through this bias optimization, the optimum operating fundamental load impedance trajectory over the frequency range for the maximum PAE point was found at $V_{\text{gs}} = -2.87$ V, where

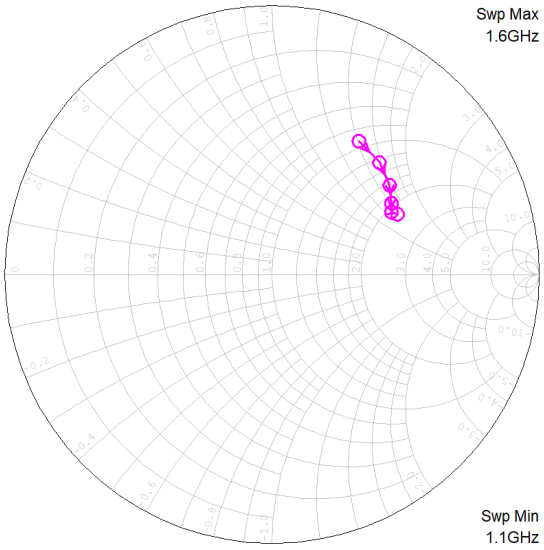

FIGURE 7. Fundamental load impedance trajectory over the frequency range for maximum PAE.

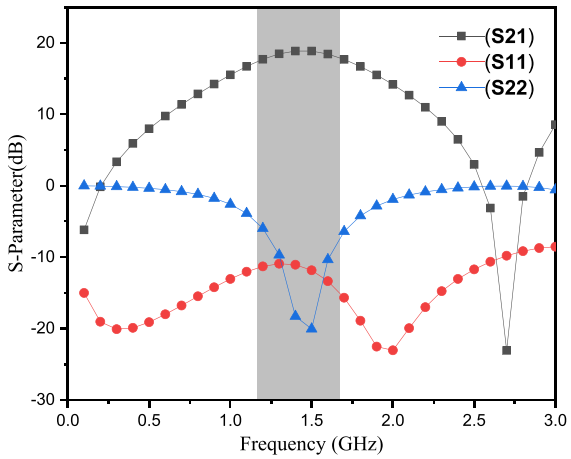

FIGURE 8. Small-signal S-parameters.

the amplifier achieved the highest combined performance in terms of PAE, P_{out}, and P_{gain}. The integration of load-pull analysis with algorithmic V_{gs} sweeping thus establishes a systematic and effective methodology for identifying the true optimum operating point, forming the foundation for enhanced efficiency in advanced high-power amplifier design [4, 31].

The output matching network is realized using RSs to further extend the amplifier's operational bandwidth and improve impedance transformation efficiency. RS introduces an optimum impedance and wideband response that effectively suppresses RF leakage into the DC bias paths while maintaining smooth impedance transformation across the 1.1–1.6 GHz range. This configuration enhances power transfer, minimizes mismatch losses, and improves harmonic suppression. Furthermore, the distributed current flow of the RS contributes to superior thermal uniformity, reducing localized heating and improving long-term device reliability. The integration of RS-based output matching with the optimized GaN device and adaptive bias control establishes a stable, efficient, and broadband amplifier architecture suitable for advanced wireless communication and electronic warfare applications [4, 32].

4. SIMULATION RESULTS AND PERFORMANCE ANALYSIS

As illustrated in Figure 8, the small-signal characterization of the proposed broadband PA confirms the accuracy of the matching network and the stability of the overall design across the 1.1–1.6 GHz frequency range.

The forward transmission coefficient (S_{21}) remains nearly constant around 20 dB, demonstrating strong and uniform gain over the entire operating band. The input reflection coefficient (S_{11}) stays below -10 dB, indicating effective input matching and minimal power reflection, while the output reflection coefficient (S_{22}) remains below -20 dB, verifying excellent output matching and load stability. These small-signal results validate the robustness of the broadband RS matching network and the effectiveness of the optimized gate-bias configuration. Overall, the amplifier exhibits wideband impedance stability and consistent gain behavior, establishing a solid foundation for high-efficiency large-signal operation.

The simulated result of the large-signal performance of the proposed broadband PA validates the effectiveness of the combined RS-based matching and gate-bias optimization approach as illustrated in Figure 9. Across the 1.16–1.6 GHz frequency range, the amplifier demonstrates stable broadband characteristics with smooth gain and efficiency profiles. At the center frequency of 1.35 GHz, the PA delivers a saturated output power (P_{out}) of 34.28 dBm while maintaining a power gain of 13.28 dB. The maximum power-added efficiency (PAE) reaches 58.69%, representing an excellent balance between broadband and efficiency.

The gain compression behavior indicates a gradual transition to saturation, verifying the amplifier's capability to handle high input drive levels without severe distortion. Moreover, the simulated PAE remains above 50% across the entire operating bandwidth, confirming the broadband nature of the matching network and the stability of the biasing scheme. All small- and large-signal simulations and performance evaluations were conducted using the AWR, ensuring accurate broadband modeling and reliable verification of the proposed design approach. Compared to conventional transmission-line-based designs, the adoption of radial stubs provides enhanced impedance bandwidth and reduced insertion loss, while the optimized V_{GS} sweep ensures operation near the optimal conduction angle.

The results demonstrate a consistent and well-balanced response, achieving high output power with excellent gain flatness and stable efficiency throughout the operational band. The amplifier delivers an average output power of approximately 34.28 dBm with a nearly constant gain of about 13.28 dB, indicating effective broadband impedance matching and minimal frequency-dependent variation. The simulated result of PAE remains above 50% across the entire band, reaching a peak value of 58.69% near the center frequency, confirming the optimized biasing and load-line conditions achieved through the

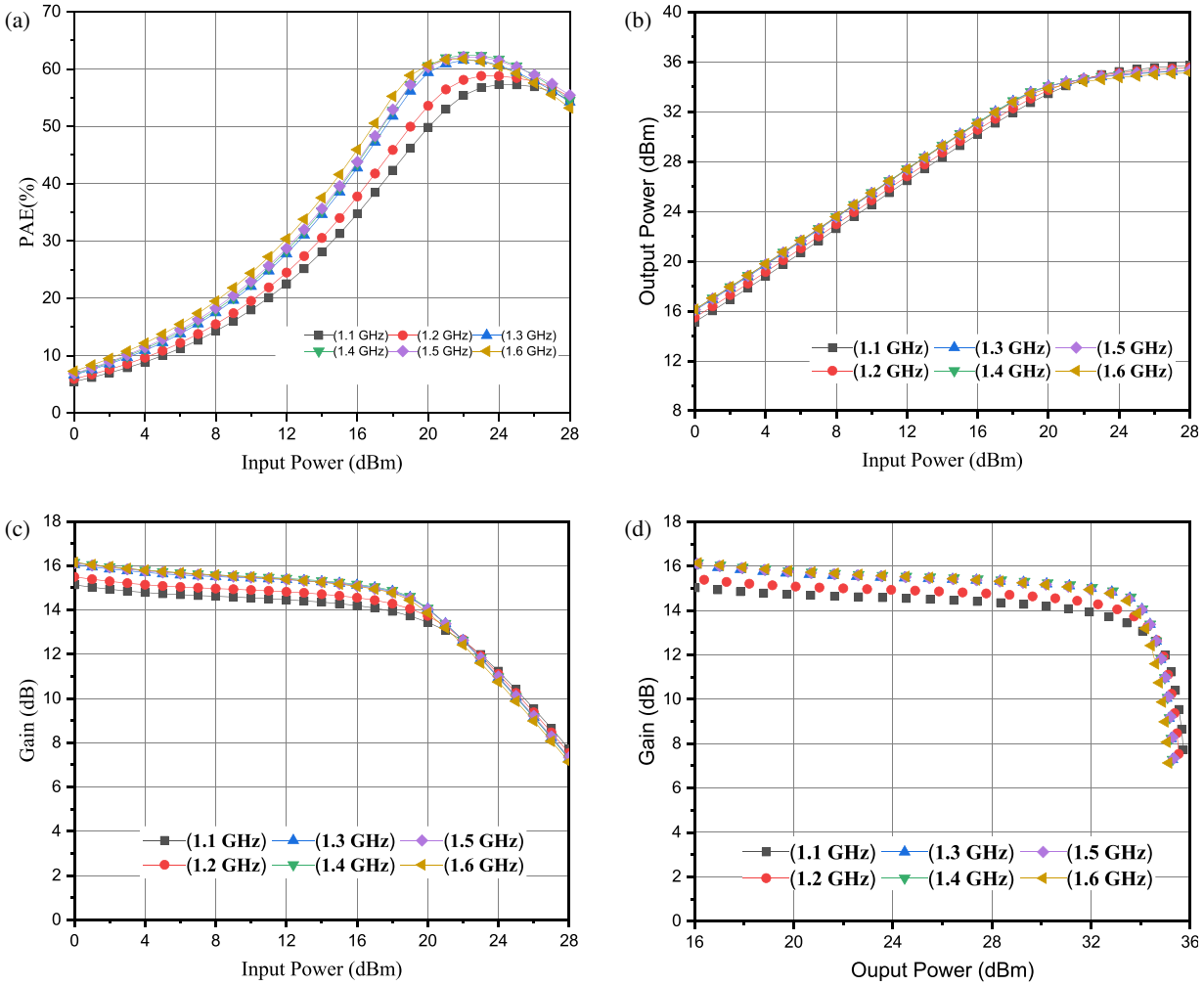

FIGURE 9. Summary of simulation results: (a) PAE versus input power, (b) P_{out} versus input power, (c) gain versus input power, and (d) power gain versus output power.

proposed gate-bias tuning approach. This flat and efficient response verifies that the CMPA0530002S GaN HEMT transistor operates within its optimal region, combining high output capability and thermal stability. The authors used Rogers 4003C as the substrate for both the matching network and bias circuit. Its key properties are: dielectric constant $\varepsilon_r = 3.75$ (nominal $\varepsilon_r = 3.66$), thickness $H = 0.508\,\text{mm}$, metal cladding $T = 0.043\,\text{mm}$, and loss tangent $\tan\delta = 0.0021$. Providing these details ensures accurate evaluation of the proposed simulation-based design. Overall, the simulated characteristics validate the effectiveness of the proposed design methodology in achieving high-efficiency, wideband performance suitable for advanced communication and electronic warfare applications.

Figure 10 presents the simulated large-signal performance of the proposed broadband PA in terms of PAE, P_{out}, and P_{gain} across the 1.16–1.6 GHz frequency range, at an input power of 21 dBm.

Overall, these results validate the robustness and repeatability of the proposed methodology, highlighting its potential for integration in high-efficiency, wideband systems used in modern communication and electronic warfare platforms.

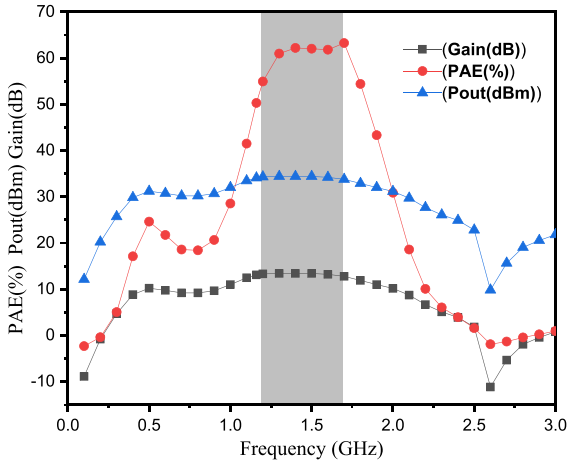

FIGURE 10. Simulated large signal results versus frequency.

4.1. Electromagnetic (EM) Modeling

Accurate electromagnetic (EM) modeling is essential for predicting and optimizing the performance of broadband power amplifiers, particularly when employing complex matching

TABLE 1. Performance comparison with state-of-the-art power amplifiers.

Paper (Ref.)	Fractional Bandwidth (%)	Center Frequency (GHz)	Saturated Output Power (dBm)	Power Added Efficiency (%)	Power Gain (dB)	Transistor Type
Hietakangas et al. [35]	2.07	1.6	33	56	13	GaAs IC
Kim et al. [36]	multi-band, per-band FBW values 3–4	low band (0.87) and high band (1.8)	34.5	55	27–28	CMOS
Refai et al. [37]	11.7	approximately 0.864	29	33–36	25–28	GaAs HBT
Alizadeh et al. [38]	17	around 10	32	50	25	GaAs pHEMT
Tang et al. [39]	33.3	approximately 6	31	36–42.7	-	GaAs HBT
Byeon et al. [40]	10.5	0.9	36	≈40	29.6	HBT
This Work	37	1.35	34.28	58.69	13.37	GaN HEMT

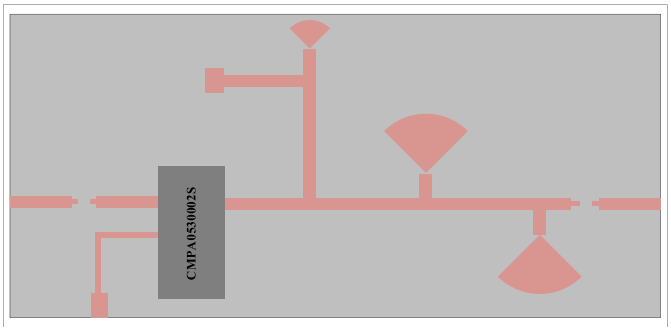

FIGURE 11. Electromagnetic (EM) modeling.

networks such as RSs. In this work, as shown in Figure 11, a full-wave EM simulation of the complete PA layout, including the output RS matching network, bias structures, and package parasitics, was conducted to capture coupling effects, discontinuities, and higher-order resonances that cannot be accounted for by lumped-element or ideal transmission-line models. The EM model enables precise extraction of S-parameters, current distributions, and field patterns, allowing simulation-based verification of impedance matching, isolation, and bandwidth performance across the 1.1–1.6 GHz operating range. By integrating EM analysis with circuit-level design and load-pull optimization, the proposed methodology ensures that the broadband PA meets its target specifications [33, 34].

To complement the schematic-level analysis, full-wave EM simulations were performed to assess the proposed PA under a more comprehensive simulation framework. This approach ensures consistency between circuit-level predictions and EM-level evaluation across the operating frequency band.

The frequency-dependent large-signal EM performance of the proposed PA is presented to assess its broadband behavior. The output power, power gain, and PAE are evaluated across the operating band at output power level of 21 dBm, as shown in Figure 12.

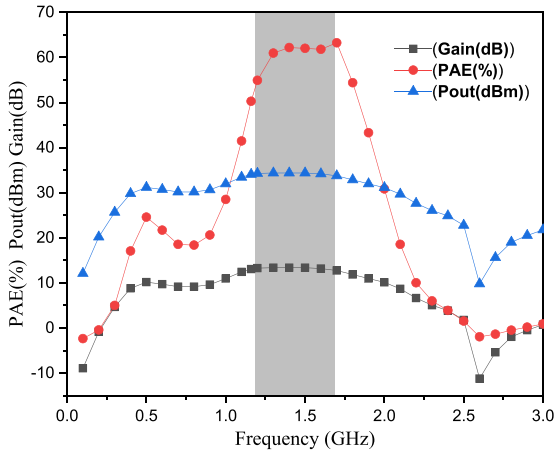

FIGURE 12. Simulated large signal results versus frequency.

5. COMPARISON OF KEY STUDIES

Table 1 compares the performance of the proposed broadband PA with recently reported state-of-the-art designs. The GaAs IC PA by Hietakangas et al. [35] achieved narrowband operation with a 2.07% FBW, 33 dBm saturated output power, and 56% PAE. The CMOS multiband PA by Kim et al. [36] provided 3–4% per-band FBW with 34.5 dBm output power, 55% PAE, and 27–28 dB gain. Refai and Davis [37] and Alizadeh et al. [38] demonstrated 11.7% and 17% FBW, respectively, achieving up to 50% PAE with GaAs HBT and pHEMT technologies. Tang et al. [39] obtained 33.3% FBW and 42.7% PAE using a GaAs HBT device, while Byeon and Kim [40] reported 10.5% FBW, 36 dBm output power, and approximately 40% PAE.

Compared with these works, the proposed GaN HEMT amplifier achieves the widest 37% FBW with a high PAE of 58.69%, 34.28 dBm saturated output power, and 13.37 dB power gain. This confirms the effectiveness of the broadband radial-stub matching network and adaptive gate-bias optimization in maintaining high efficiency and output power across a wide operating band.

6. CONCLUSION

This paper has introduced a holistic design framework for broadband GaN HEMT power amplifiers, which combines radial-stub-based bias and output matching networks with automated gate-bias optimization and load-pull termination analysis. Applied to the CMPA0530002S device, the resulting amplifier delivered 34.28 dBm saturated output power, a flat gain of approximately 13.28 dB, and a peak power-added efficiency (PAE) of 58.69% across a 1.1–1.6 GHz band (37% FBW), where its broadband and high-efficiency characteristics provide significant advantages for electronic-warfare and precision-navigation systems. These simulation results demonstrate that the coordinated tuning of bias, impedance, and matching network topology can effectively reconcile the traditional trade-offs among bandwidth, efficiency, and output power in PA design.

Moreover, the radial-stub topology demonstrated excellent effectiveness in achieving broadband impedance uniformity with high efficiency, and the algorithmic V_{GS} sweep enabled broadband efficiency optimization without the need for manual tuning. Although this paper focuses on a single-stage PA in the 1 GHz band, the proposed methodology is equally applicable to multi-stage, Doherty, or outphasing architectures and scalable to higher frequencies for next-generation wireless and electronic-warfare systems. Future work will involve detailed linearity and modulation-mask testing, ruggedized commercial packaging, and implementation in millimeter-wave frequencies.

The presented EM-validated layout represents the final fabrication-ready design, and hardware implementation and measurements are planned as a part of ongoing work. Future work will focus on the fabrication and experimental characterization of the proposed PA, enabling a detailed comparison between measured and simulated large-signal performance.

REFERENCES

[1] Naik, G., J.-M. Park, J. Ashdown, and W. Lehr, "Next generation Wi-Fi and 5G NR-U in the 6 GHz bands: Opportunities and challenges," *IEEE Access*, Vol. 8, 153 027–153 056, 2020.

[2] Mabrok, M., Z. Zakaria, and N. Saifullah, "Design of wide-band power amplifier based on power combiner technique with low intermodulation distortion," *International Journal of Electrical and Computer Engineering (IJECE)*, Vol. 8, No. 5, 3504–3511, Oct. 2018.

[3] Erunkulu, O. O., A. M. Zungeru, C. K. Lebekwe, M. Mosalaosi, and J. M. Chuma, "5G mobile communication applications: A survey and comparison of use cases," *IEEE Access*, Vol. 9, 97 251–97 295, 2021.

[4] Cripps, S. C., *RF Power Amplifiers for Wireless Communications*, 2nd ed., Artech House, Norwood, MA, 2006.

[5] Amar, A. S. I., M. Mamidanna, M. Darwish, and H. El-Hennawy, "High gain broadband power amplifier design based on integrated diplexing networks," *IEEE Microwave and Wireless Components Letters*, Vol. 32, No. 2, 133–136, Feb. 2022.

[6] Cai, Q., W. Che, and Q. Xue, "High-efficiency power amplifier with a multiharmonic tuning network," *IEEE Microwave and Wireless Components Letters*, Vol. 31, No. 4, 389–392, Apr. 2021.

[7] Feng, W., W. Wu, X. Y. Zhou, W. Che, and Y. Shi, "Broadband high-efficiency quasi-Class-J power amplifier based on nonlinear output capacitance effect," *IEEE Transactions on Circuits and Systems II: Express Briefs*, Vol. 69, No. 4, 2091–2095, 2022.

[8] Sun, J. X., F. Lin, B. Li, H. Sun, and W. Chen, "Continuous Class-J/F^{-1} mode asymmetrical Doherty power amplifier with extended bandwidth and enhanced efficiency," *IEEE Transactions on Microwave Theory and Techniques*, Vol. 71, No. 11, 4814–4825, Nov. 2023.

[9] Sheikhi, A., "Historical aspect of load-modulated balanced amplifiers," *IEEE Access*, Vol. 12, 7974–7986, 2024.

[10] Nikandish, G., R. B. Staszewski, and A. Zhu, "Breaking the bandwidth limit: A review of broadband Doherty power amplifier design for 5G," *IEEE Microwave Magazine*, Vol. 21, No. 4, 57–75, 2020.

[11] Mabrok, M., Z. Zakaria, T. Sutikno, and A. Alhegazi, "Wideband power amplifier based on Wilkinson power divider for S-band satellite communications," *Bulletin of Electrical Engineering and Informatics*, Vol. 8, No. 4, 1531–1536, 2019.

[12] Boumalkha, M., A. G. Abdellatif, A. S. I. Amar, M. Lahsaini, A. Almslmany, S. Ansari, M. Alammar, and M. A. Shawky, "Investigating broadband filtering power amplifier using multi-mode resonator-based bandpass filter," *Results in Engineering*, Vol. 26, 105035, 2025.

[13] Sayed, A., S. Preis, and G. Boeck, "Efficient technique for ultra broadband, linear power amplifier design," *International Journal of Microwave and Wireless Technologies*, Vol. 4, No. 6, 559–567, 2012.

[14] Cwikliński, M., C. Friesicke, P. Brückner, D. Schwantuschke, S. Wagner, R. Lozar, H. Maßler, R. Quay, and O. Ambacher, "Full W-band GaN power amplifier MMICs using a novel type of broadband radial stub," *IEEE Transactions on Microwave Theory and Techniques*, Vol. 66, No. 12, 5664–5675, 2018.

[15] Wang, Z. and C.-W. Park, "Novel wideband GaN HEMT power amplifier using microstrip radial stub to suppress harmonics," in *2012 IEEE/MTT-S International Microwave Symposium Digest*, 1–3, Montreal, QC, Canada, Jun. 2012.

[16] Mustafa, S. M., M. Hayati, M. Khodadoost, S. A. Sadeq, F. Shama, and P. Karami, "Compact microstrip lowpass filter with wide stopband and sharp transition band using radial stub resonator," *AEU — International Journal of Electronics and Communications*, Vol. 186, 155468, 2024.

[17] Wan, F., Y. Xu, and B. Ravelo, "Radial stub based negative group delay circuit theory," *IET Microwaves, Antennas & Propagation*, Vol. 14, No. 6, 515–521, 2020.

[18] Zhao, J., S. Wang, X. Chen, W. Lv, Z. Li, and H. Jiang, "Miniaturized microstrip branch-line coupler with wideband harmonic suppression using modified radial stub loaded resonators," in *2023 15th International Conference on Communication Software and Networks (ICCSN)*, 358–360, Shenyang, China, Jul. 2023.

[19] Wang, Z. and C.-W. Park, "Novel wideband high-efficiency high-power amplifier using microstrip radial stub for 4G communication systems," *Microwave and Optical Technology Letters*, Vol. 56, No. 6, 1412–1418, Jun. 2014.

[20] Vardhan, S. H., D. Pathak, R. Ramalingam, M. Mehnde, and A. Dutta, "Microstrip radial stub based 4W GaN MMIC power amplifier for X-band radar applications," in *2021 International Conference on Advances in Electrical, Computing, Communication and Sustainable Technologies (ICAECT)*, 1–4, Bhilai, India, Feb. 2021.

[21] Mohammadi, B., J. Nourinia, C. Ghobadi, and A. Valizade, "Design and analysis of the stub and radial-stub loaded resonator band-pass filter with cross-shaped coupled feed-lines for UWB

applications," *Applied Computational Electromagnetics Society Journal (ACES)*, Vol. 28, No. 9, 851–857, 2021.

[22] Sharifi, M. and V. Mashayekhi, "Design of a modified hairpin bandpass filter using embedded radial stubs featuring ultrawide stopband," *AEU — International Journal of Electronics and Communications*, Vol. 164, 154624, 2023.

[23] Kwon, H., H. Lim, and B. Kang, "Design of 6–18 GHz wideband phase shifters using radial stubs," *IEEE Microwave and Wireless Components Letters*, Vol. 17, No. 3, 205–207, Mar. 2007.

[24] Singh, P. K., A. K. Tiwary, and N. Gupta, "Design of radial microstrip band pass filter with wide stop-band characteristics for GPS application," *Progress In Electromagnetics Research C*, Vol. 59, 127–134, 2015.

[25] Nguyen, D. P., X.-T. Tran, N. L. K. Nguyen, P. T. Nguyen, and A.-V. Pham, "A wideband high efficiency Ka-band MMIC power amplifier for 5G wireless communications," in *2019 IEEE International Symposium on Circuits and Systems (ISCAS)*, 1–5, Sapporo, Japan, May 2019.

[26] Mohamed, E. N., A. M. E. Abounemra, M. Darwish, and A. M. El-Tager, "A generic multidimensional design methodology for highly efficient RF power amplifier with improved linearity," *IEEE Transactions on Microwave Theory and Techniques*, Vol. 72, No. 11, 6401–6413, 2024.

[27] Tan, J., K. S. Yuk, and G. R. Branner, "Design of a high power, wideband power amplifier using AlGaN/GaN HEMT," in *2017 IEEE 18th Wireless and Microwave Technology Conference (WAMICON)*, 1–4, Cocoa Beach, FL, USA, Apr. 2017.

[28] Smorynski, C., *MVT: A Most Valuable Theorem*, Springer, 2017.

[29] Kim, J., "A review of Ku-band GaN HEMT power amplifiers development," *Micromachines*, Vol. 15, No. 11, 1381, 2024.

[30] Pozar, D. M., *Microwave Engineering*, 4th ed., John Wiley & Sons, Hoboken, NJ, 2012.

[31] Boshnakov, I., "Designing power amplifiers using maximum-efficiency lines and constant power contours," *High Frequency Electronics*, Vol. 18, No. 6, 28–34, Jun. 2019.

[32] Bahl, I., *Fundamentals of RF and Microwave Transistor Amplifiers*, 1st ed., John Wiley & Sons, Hoboken, NJ, 2009.

[33] Gonzalez, G., *Microwave Transistor Amplifiers: Analysis and Design*, 2nd ed., Prentice Hall, Upper Saddle River, NJ, 1996.

[34] Merza, M. E. and K. K. Mohamed, "Design and optimization of the GaN HEMT Class-J power amplifier for 2.4 GHz applications," in *2024 21st International Multi-Conference on Systems, Signals & Devices (SSD)*, 509–518, Erbil, Iraq, 2024.

[35] Hietakangas, S., J. Typpo, and T. Rahkonen, "Integrated 1.6 GHz, 2W tuned RF power amplifier," in *2008 NORCHIP*, 176–179, Tallinn, Estonia, 2008.

[36] Kim, W., K. S. Yang, J. Han, J. J. Chang, and C. H. Lee, "An EDGE/GSM quad-band CMOS power amplifier," *IEEE Journal of Solid-State Circuits*, Vol. 49, No. 10, 2141–2149, Oct. 2014.

[37] Refai, W. Y. and W. A. Davis, "A highly efficient linear multimode multiband Class-J power amplifier utilizing GaAs HBT for handset modules," *IEEE Transactions on Microwave Theory and Techniques*, Vol. 68, No. 8, 3519–3531, 2020.

[38] Alizadeh, A., S. Hassanzadehyamchi, A. Medi, and S. Kiaei, "An X-band Class-J power amplifier with active load modulation to boost drain efficiency," *IEEE Transactions on Circuits and Systems I: Regular Papers*, Vol. 67, No. 10, 3364–3377, Oct. 2020.

[39] Tang, W., L. Peng, S. Lin, G. Zhang, and Z. Zhang, "A broadband high efficiency Class-J power amplifier for C-band," *Microwave Journal*, May 2023.

[40] Byeon, C.-W. and J.-H. Kim, "2W HBT power amplifier module with dual second harmonic suppression technique," *Sensors*, Vol. 25, No. 4, 1231, Feb. 2025.